INDIRECT CONTROL OF A SINGLE-PHASE ACTIVE POWER FILTER

Emil Rosu, Mihai Culea, Teodor Dumitriu, and Traian Munteanu

"Dunarea de Jos" University, Galati, Romania

Abstract: The control of shunt active power filters using PWM inverters consists in generating a reference by separating, using different methods, the harmonics to be eliminated. The methods used are time-consuming and need dedicated control and signal processing equipments. To avoid these setbacks a new method is proposed in the paper. The active power filter is a current PWM rectifier with voltage output and with a capacitor on the DC side. The PWM rectifier is controlled so that the sum of its current and the load's current is a sinusoid. The control block as well as simulation results are presented.

Keywords: Active power filters, PWM rectifiers, hysteresis control, THD.

1. INTRODUCTION

The classical structure of a single phase APF using a voltage inverter is presented in Fig. 1, where SD is a non-linear load. The APF is injecting a current so that the total current drawn from the mains

$$(1)\ \ i_R(t) = i_S(t) - i_F(t)$$

is sinusoidal and the voltage and current phases are identical.

The APF's current is

$$(2)\ \ i_F(t) = \tilde{i}_S(t) = i_S(t) - i_S^1(t)$$

where $i_S^1(t)$ is is the fundamental and $\tilde{i}_S(t)$ is the sum of higher order harmonics, often named the polluting component.

Separation of the polluting current component from the fundamental is a rather complicated procedure. In (Ionescu, *et all*, 1998) some of these methods are presented, such as the instantaneous powers method or the filtering of the components. Several other methods are presented in literature but they are usually application oriented.

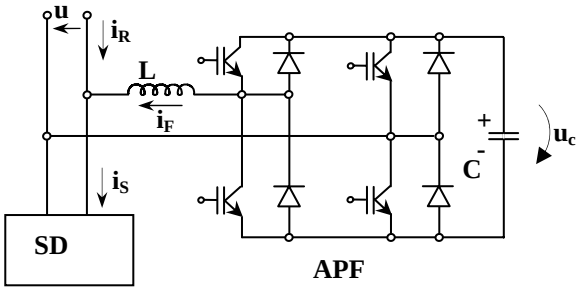

Fig.1. APF structure.

A new approach, called indirect control, is presented. The application does not need a prior knowledge of the non-linear load's current spectrum.

The schematic of the system is presented in Fig. 2. Unlike the classical structure, the supply of the load and of the APF is done through the inductor L in a structure specific to PWM current rectfier with voltage output.

This paper was recommended for publication by Emil Ceanga

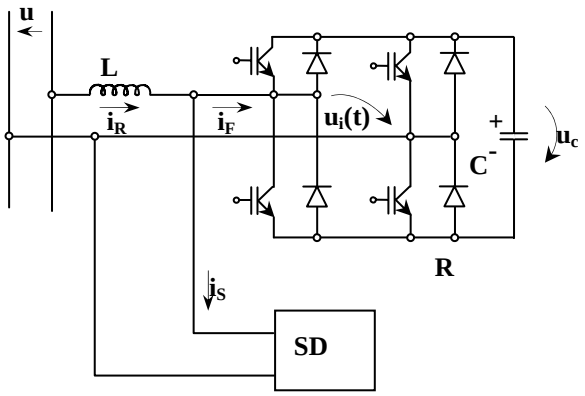

Fig.2. Indirect control structure.

The current drawn from the mains is

$$(3)\ \ i_R(t) = i_S(t) + i_F(t)$$

To obtain a sinusoidal form the current drawn by the rectifier should be

$$(4)\ \ i_F(t) = i_F^1(t) + \tilde{i}_F(t)$$

where $i_F^1(t)$ is the fundamental current used to keep the capacitor C charged while for the harmonic components of the current the following holds out

$$(5)\ \ \tilde{i}_F(t) + \tilde{i}_S(t) = i(t)$$

where $i(t)$ is the fundamental in phase with the mains voltage. By using (3), (4), and (5) the total drawn current is

$$(6)\ \ i_R(t) = i_F^1(t) + i_S^1(t) + i(t)$$

The sum of the current drawn by the rectifier and the load is a sinusoidal current at the point of common coupling in phase with the voltage.

Considering the structure of the PWM control $i_R(t)$ will contain a minimum higher order harmonics while keeping the phase shift to a minimum.

2. CONTROL STRATEGIES

Different control strategies, such as open-loop sinusoidal PWM, open or closed loop hysteresis control can be used. The amplitude modulation index m_A has to be determined for the sinusoidal PWM control following

$$(7)\ \ m_A = \frac{\sqrt{2}U_i}{U_C}$$

where the input voltage of the PWM rectifier is

$$(8)\ \ u_i(t) = \sqrt{2}U_i \sin(\omega t + \varphi)$$

the mains voltage

$$(9)\ \ u(t) = \sqrt{2}U \sin(\omega t)$$

and the total drawn current

$$(10)\ \ i_R(t) = \sqrt{2}I_R \sin(\omega t)$$

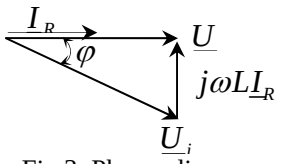

Fig.3. Phasor diagram.

This can be represented on a phasor diagram as in Fig.3. By using linear modulation, $m_A \le 1$, the boost characteristic of the rectifier is obvious and the phase is

$$(11)\ \ \varphi = \text{arc}tg\frac{\omega L I_R}{U}$$

The RMS value of the current is determined based on the sum of active powers which can be written as

$$(12)\ \ U.I_R = U.I_S^1 + C.U_C\frac{\Delta U_C}{T}$$

where ΔU_C and T are the capacitor voltage ripple and period.

From (12) it can be observed that the capacitor voltage can be determined and the RMS of the load current has to be determined, which is a major setback. Moreover, for any change in the load the RMS has to be recalculated. For the open-loop hysteresis control the problem is similar but the RMS value to be calculated is for I_R. The closed loop hysteresis control is presented in Fig. 4.

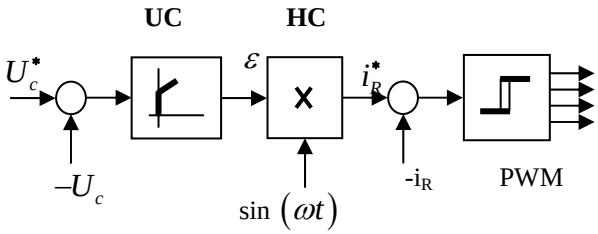

Fig.4. Control structure.

The choice of U_C as a controlled value is determined by the boost characteristics of the rectifier which determined by the value of the U_i produces variations of the output. The error of the output voltage is transformed into a reference for the input current

$$(13)\ \ i_R^* = \varepsilon.\sin(\omega t)$$

which has the same phase as the mains voltage. The current is controlled using a hysteresis controller HC

having an acceptable hysteresis band relating to the current ripple and switching frequency.

3. SIMULATION MODEL

To validate the proposed control scheme the model presented in Fig. 5 was used. A single phase rectifier with a capacitive filter was considered due to the fact that it is highly non-linear. The input voltage and current are presented in Fig. 6 for the case of a $1000\mu F$ capacitor, a $10mH$ inductor filter and a 10Ω load. The THD coefficient of the current is 28.27 %.

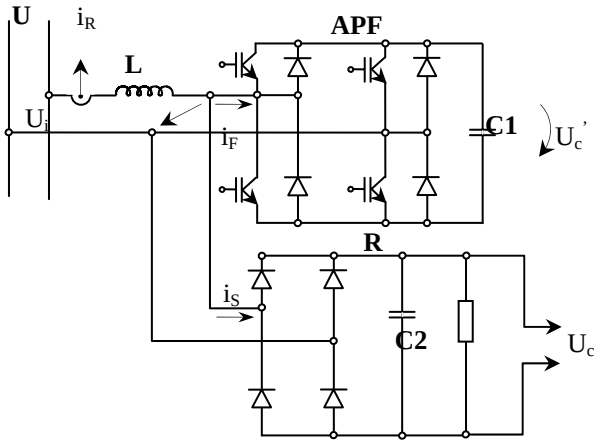

Fig.5. Simulation model.

4. EXPERIMENTAL RESULTS

The model was used to simulate, via SIMULINK, different conditions, taking into account the dynamic of the system, THD coefficient and the output voltage. The mains voltage and current variations are presented in Fig. 7 for a reference of 110V for the output voltage. The dynamic response has about two periods and the THD is reduced to 3.54% while the ripple is very small.

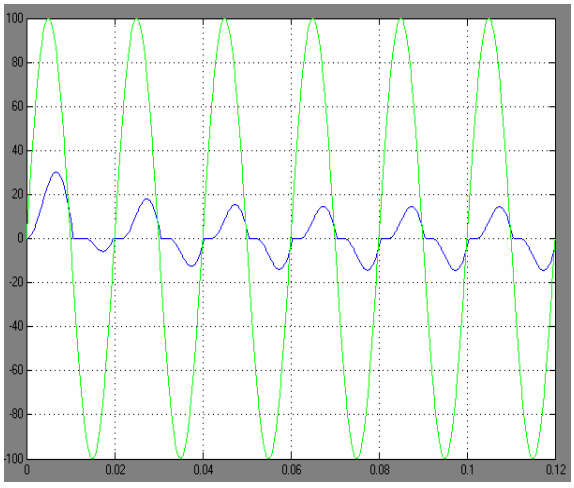

Fig.6. Uncontrolled rectifier current and voltage

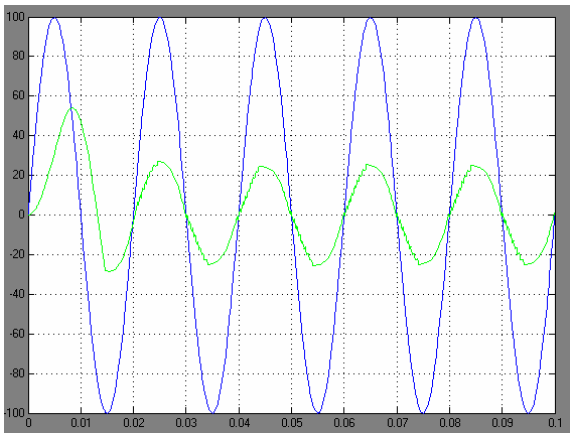

Fig.7. Input current and voltage, U_C=110V

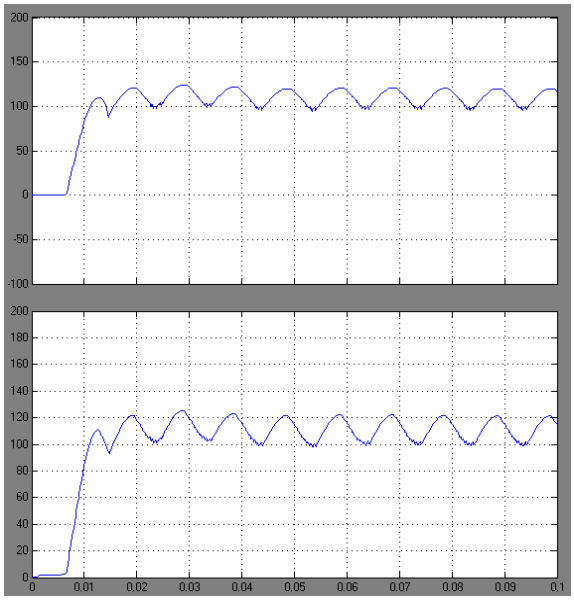

Fig.8. U'_C and U_C voltages, U_C=110V

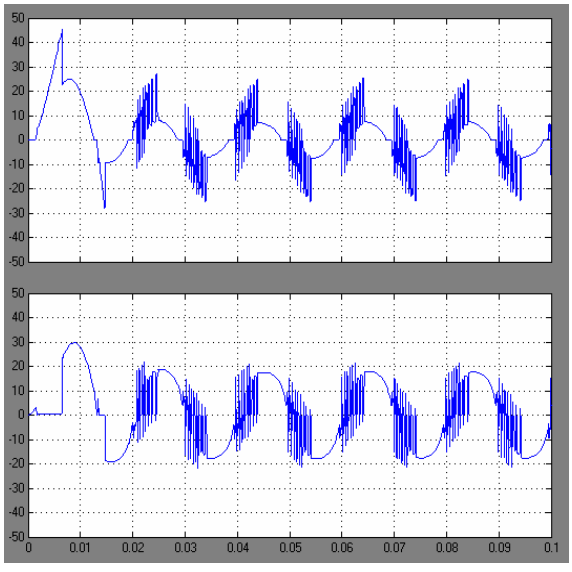

Fig.9. Filter and load currents, U_C=110V

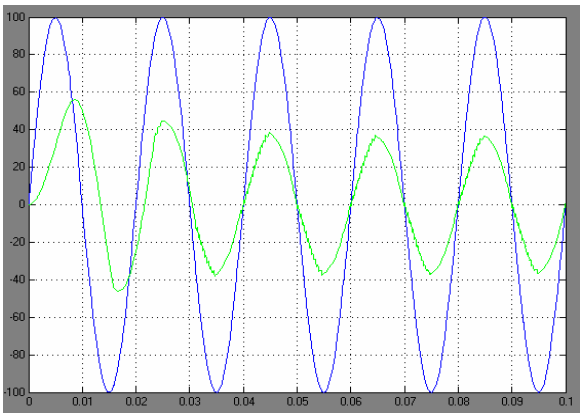

Fig.10. Input current and voltage, U_C=130V

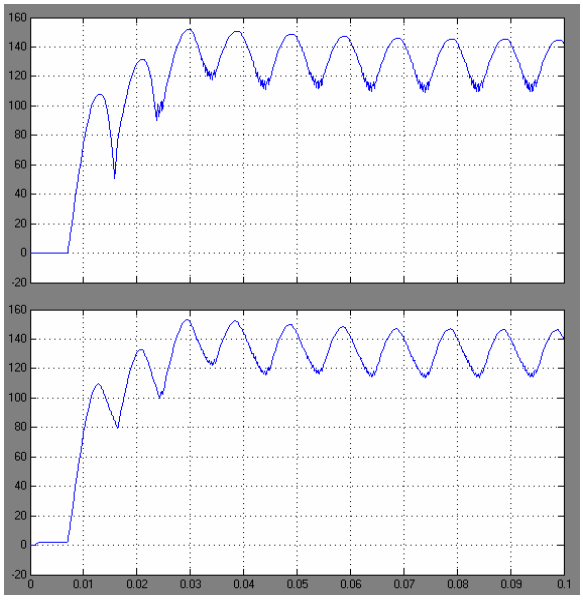

Fig.11. U'_C and U_C voltages, U_C=130V

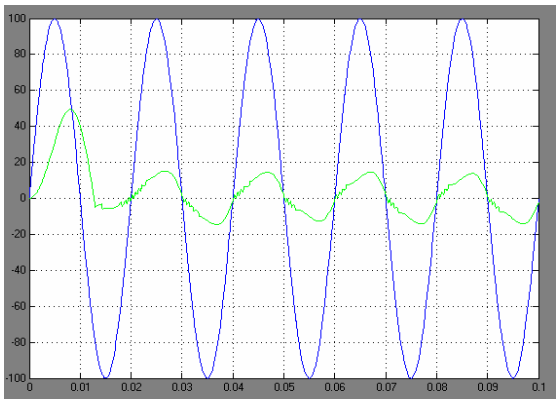

Fig.12. Input current and voltage, U_C=80V

The output voltages for the PWM rectifier and the load have the same average value of 110V since they are both powered from the same supply, $u_i(t)$, and are presented in Fig. 8. They also outline the boosting characteristic of the rectifier, the output of the load being higher than usual. The voltage ripple is typical for the filter used. The input currents filter and load, are presented in Fig. 9.

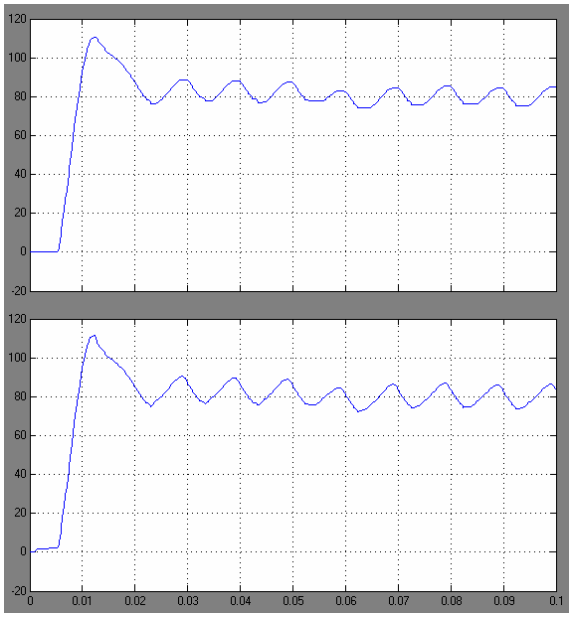

Fig.13. U'_C and U_C voltages, U_C=80V

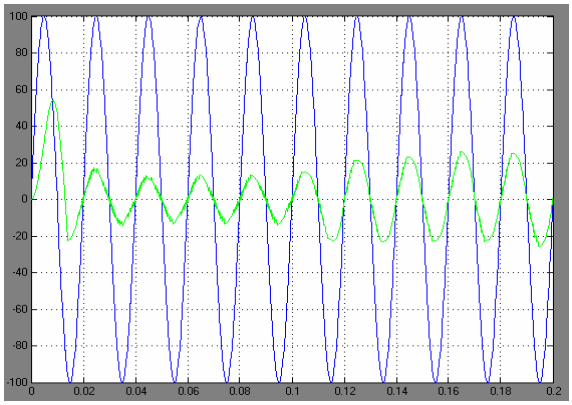

Fig.14. Input current and voltage

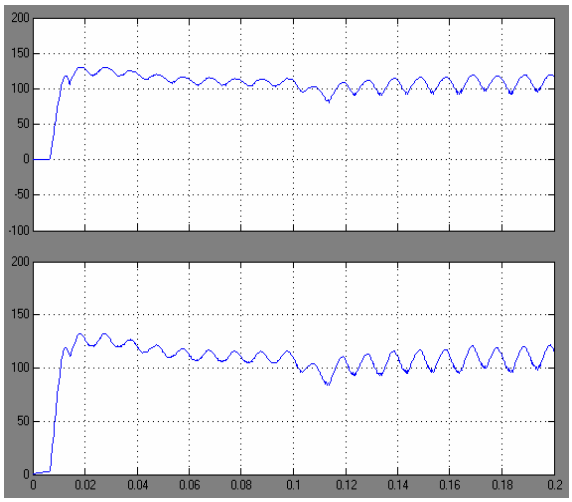

Fig.15. U'_C and U_C voltages

The influence of the PWM rectifier and hysteresis control can be noticed on the first half of a semi-period when usually the current of the load rectifier is zero. In the second half of the semi-period when the current is sinusoidal, the APF does not work as the PWM rectifier, but it is functioning as an uncontrolled rectifier. There is also a supplementary conduction through the uncontrolled rectifier, determined by the variation of $u_i(t)$ and the boosting character of the ensemble. While the oscillations of the currents are important, they don't appear in the input current or in the output voltages. A second simulation test was carried out for a 130V reference. The results are presented in Fig. 10, the input voltage and current, and in Fig. 11, the output voltages. The same conclusions apply and THD = 3.3%. The third simulation test, Fig.12 and 13, was done using a 80V reference, for an amplitude modulation coefficient

$$(14)\quad m_A = \frac{\sqrt{2}U_i}{U_C} \cong \frac{\sqrt{2}U}{U_C} = \frac{100}{80} > 1$$

The output voltages follow the reference as expected, but there are larger values for the higher harmonics and THD = 8.73 %. This behaviour is determined by the over-modulation which induced nonlinearities in the control.

The fourth test also considered the variation of the load from 20Ω to 10Ω at t=0.1 sec. The input current and voltage are presented in Fig. 14 and the output voltages in Fig. 15. There are two differences, as for the 20Ω load the PWM is extended to a semi-period due to a reduced current, while for the 10Ω load the operation is similar to the one presented afore. The output voltages follow the reference after a short transient regime.

An interesting behaviour can be observed when the supply voltage *u(f)* is distorted with 5th and 7th harmonic. This can be written as:

$$(15)\quad u(t) = \sqrt{2}U_1 \sin(100\pi t) + \sqrt{2}U_5 \sin(500\pi t) + \sqrt{2}U_7 \sin(700\pi t).$$

Simulations were carried out for different values of supply voltage THD factor and the results are presented in Table I. For small THD factors there is an decrease of the THD which can be explained based on the 5th and 7th harmonics drawn by the nonlinear load. For large values of the mains voltage THD the current is also distorted, the THD factor beeing almost double which indicates the limitations of the method. However, this case is unlikely to be a real one, since such large values for the THD are uncommon.

Mains voltage variations are presented in figure 16 as well as the current drawn from the mains, illustrating the second case presented in Table I

Table 1 The influence of mains voltage THD on the behaviour of the APF

$\sqrt{2}U_1$	$\sqrt{2}U_5$	$\sqrt{2}U_7$	$THD-u$	$THD-i_R$
100	7	5	8.6 %	3.20 %
100	10	7	12.2%	3.44 %
100	20	10	22.36 %	8.72 %

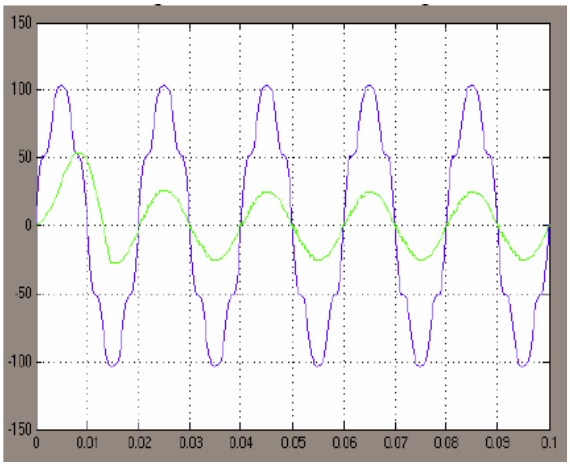

Fig.16. Input current and voltage

The dynamic of the system is tested by switching from a sinusoidal to a distorted mains voltage. A distorted voltage is applied at *t*=0.8 sec and the system is responding instantaneously, as it can be seen from the THD of the current, showing robustness to mains voltage distortions.

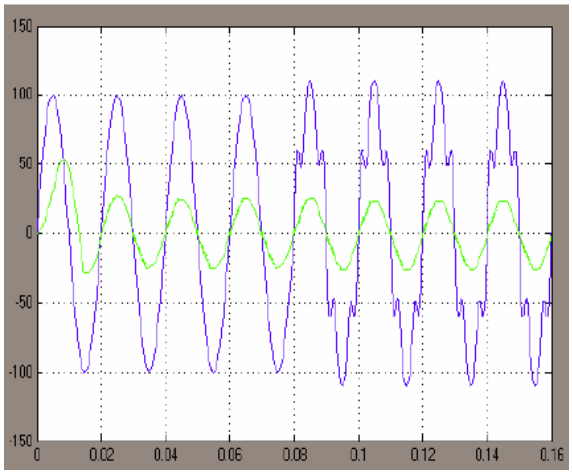

Fig.17. Input current and voltage

Simulations were also carried out to evaluate the influence of the voltage amplitude variation on the system. A 5% voltage drop did not influence the output voltage U_C which kept the 110V reference value, while the output of the PWM inverter is not significantly influenced as in fig.18. Therefore the proposed system has also a voltage control effect due to the closed loop control.

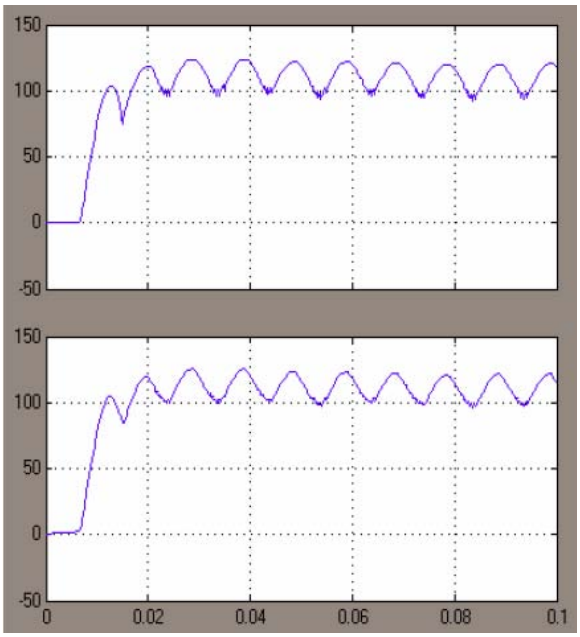

Fig.18. U'_C and U_C voltages

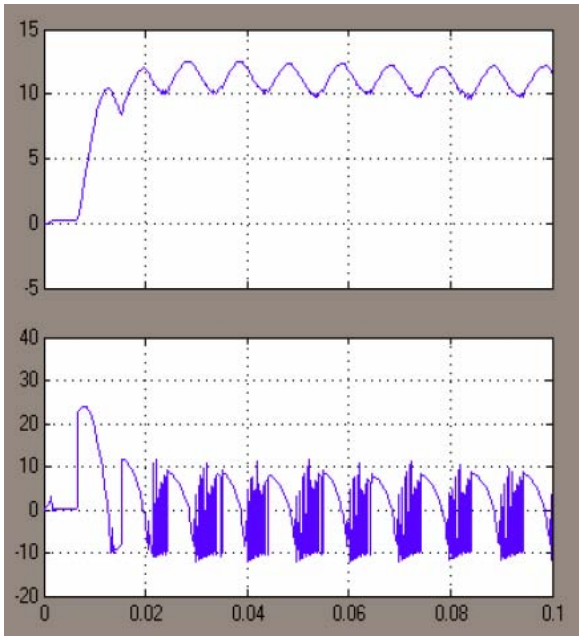

Fig.19. Load and capacitor C_2 currents

An important issue is the shape of the current $i_S(t)$ drawn by the nonlinear load SD, given by:

$$(16)\quad i_S(t) = i_{C2}(t) + i_L(t)$$

where $i_L(t)$ is the load current and $i_{C2}(t)$ is the current passing through the filtering capacitor. The currents are presented in figure 19. The load current is not influenced by the PWM control but the filtering capacitor is oversolicited by the high order harmonics generated by the PWM rectifier.

The controller for the output voltage, UC, is a PI controller with an experimental parameters adjusting..

A $\pm 0.5A$ hysteresis band was considered for the current control, leading to a switching frequency of up to 5 kHZ. Reducing the hysteresis band will indeed reduce the THD but the improvement is limited and determines an increase of the switching frequency

5. CONCLUSIONS

The simulated results prove that the proposed structure is operating accordingly. The substantial decrease of the THD recommends the solution as a viable option with good performances. The solution can also be applied for controlled rectifiers which will allow the control of the output voltage.

The main drawback is the presence of the inductor of relatively large value that depends on the output voltage; however, this also applies to all the other APF structures. The inductor has to be designed to withstand the currents from the rectifier and also the PWM rectifier.

The solution can also be applied to three-phase rectifiers since the harmonics are greatly reduced.

6. REFERENCES

H. Akagi, "New Trends in Active Filters for Power Conditioning", IEEE Transactions, 1996, IA-32.

F. Ionescu, S. Nitu, E. Rosu, "Preocupari actuale in domeniul electronicii de putere", Editura SECOREX, ISBN 973-85298-3-2, Bucuresti 2001.

F. Ionescu, D. Floricau, S. Nitu, J.P.Six. Ph. Delarue, C. Bogus, "Electronica de putere. Convertoare statice" , Editura Tehnica, ISBN 973-31-1262-3, Bucuresti 1998.

T. E. Nunez-Zuninga and J.A. Pomilio, "Shunt Active Power Filter Synthesizing Reisitive Loads", IEEE Transactions in Power Electronics, vol.17, No 2, March 2002.